

Survivability of Moon Systems Around Ejected Gas Giants

Ian Rabago¹ and Jason H. Steffen¹^{*}

¹*University of Nevada, Las Vegas*

Accepted XXX. Received YYY; in original form ZZZ

ABSTRACT

We examine the effects that planetary encounters have on the moon systems of ejected gas giant planets. We conduct a suite of numerical simulations of planetary systems containing three Jupiter-mass planets (with the innermost planet at 3 AU) up to the point where a planet is ejected from the system. The ejected planet has an initial system of 100 test-particle moons. We determine the survival probability of moons at different distances from their host planet, measure the final distribution of orbital elements, examine the stability of resonant configurations, and characterize the properties of moons that are stripped from the planets. We find that moons are likely to survive in orbits with semi-major axes out beyond 200 planetary radii (0.1 AU in our case). The orbital inclinations and eccentricities of the surviving moons are broadly distributed and include nearly hyperbolic orbits and retrograde orbits. We find that a large fraction of moons in two-body and three-body mean-motion resonances also survive planetary ejection with the resonance intact. The moon-planet interactions, especially in the presence of mean-motion resonance, can keep the interior of the moons molten for billions of years via tidal flexing, as is seen in the moons of the gas giant planets in the solar system. Given the possibility that life may exist in the subsurface ocean of the Galilean satellite Europa, these results have implications for life on the moons of rogue planets—planets that drift through the galaxy with no host star.

Key words: planets and satellites: dynamical evolution and stability – methods: numerical – planet-star interactions

1 INTRODUCTION

Of the locations where we imagine finding evidence for life in the solar system, only one is in the traditional “habitable zone” where liquid water exists on the surface due to solar radiation. Another promising place to imagine finding life is on water-rich moons of the giant planets—with Europa being the most prominent (Squyres et al. 1983; Sparks et al. 2017). These moons do not reside (and likely have never resided) within the canonical habitable zone of the Sun. The energy that keeps their subsurface water in liquid form comes from tidal flexing due to the moons’ orbital eccentricity and their relatively close proximity to their host planet (Vance et al. 2018; Reynolds et al. 1987). The conditions that provide the energy needed to sustain the liquid water layers have persisted for billions of years in the solar system and are expected to continue for billions more (Yoder & Peale 1981). Thus, when considering the possibility for life outside the solar system, the moons of gas giant planets are a plausible candidate location (Hinkel & Kane 2013; Forgan & Kipping 2013; Lammer et al. 2014; Zollinger et al. 2017).

During star formation, systems frequently produce multiple gas giant planets, as seen by Doppler surveys (Knutson et al. 2014; Schlaufman & Winn 2016). Once the protoplanetary disk dissipates, many of these systems will be unstable. Dynamical interactions among the planets would lead to the ejection of one or more planets from the system. Indeed, this scenario is a prominent theory for the formation of hot Jupiter systems (Rasio & Ford 1996; Chatterjee et al. 2008) where the encounter that ejects one gas giant simultaneously leaves the remaining planet on a highly eccentric orbit—which then circularizes under the dissipative effects of tidal flexing (Goldreich & Soter 1966). The final orbit will be at a distance one to two times the original pericenter distance (from conservation of angular momentum while the orbital energy dissipates).

If this mechanism does produce the hot Jupiter population, or a sizeable portion of it, it would simultaneously generate a population of “rogue planets”, ejected from the system to wander the galaxy without a stellar host. There is some evidence from microlensing searches for the existence of such rogue planets—perhaps numbering in the billions (Sumi et al. 2011; Bennett et al. 2014). If these rogue planets can retain their moons throughout the dynamical en-

* E-mail: jason.steffen@unlv.edu

counters that lead to their ejection from their home system, then some of those moons may bring with them substantial reservoirs of liquid water. As is the case in the solar system, the liquid state of this water may persist for billions of years through tidal interactions with the host planet. Thus, if the moons can survive, it may be possible for life to exist around these planets even in the absence of radiation from a nearby star.

In this work, we use a suite of N-body simulations to estimate the probability of moons surviving in orbit around ejected gas giant planets, and examine some of their anticipated orbital properties. The paper is organized as follows. In Section 2 we detail 77 numerical simulations involving dynamically unstable gas giant systems, and then examine the results of those simulations in Section 3. We briefly compare our results with those of [Hong et al. \(2018\)](#)—a related study that we became aware of as we were preparing this work. Finally, we discuss some of the broader implications of our results and give our conclusions.

2 SIMULATION SETUP

Our initial systems comprise three Jupiter-mass planets orbiting a solar-mass star. We assume each planet has a Jupiter radius R_J , although this will not play a role in the integration. The innermost planet is assigned a semi-major axis of 3 AU. The semi-major axes of the remaining planets are assigned by assigning the orbital period of each planet to be a random ratio with its interior neighbor. The random ratios are uniformly distributed between 1.2 and 1.4. The eccentricities e and orbital inclinations i (in radians) of the three planets are drawn from a Rayleigh distribution with a Rayleigh parameter of 0.01. The longitude of pericenter ϖ , longitude of ascending node Ω , and the mean anomaly M are all uniformly distributed between 0 and 2π .

Once the initial setup is complete, we integrate the systems using the IAS15 adaptive integrator in the REBOUND software package ([Rein & Liu 2012](#); [Rein & Spiegel 2015](#)). The systems evolve until either a planet is ejected or until a maximum time of 10 Myrs is reached. Our criterion for planet ejection is when the planet reaches an orbital distance greater than 100 AU. Most systems eject a planet very quickly due to the close proximity of the neighboring planets.

Once a planet is ejected from its system, the planet in question is identified and the simulation is restarted at an earlier time using the Simulation Archive feature of REBOUND ([Rein & Tamayo 2017](#)). The time chosen for the restart is 10 million days prior to the final ejection time (roughly $\frac{1}{300}$ of the maximum allowed simulation time) or from the beginning if the simulation time is shorter. We add a set of 100 massless moons in circular orbits around the identified planet with the first moon at a distance of $2R_J$ from the planet (about one third the orbital distance of Io around Jupiter). Each subsequent moon is placed an additional $2R_J$ outwards. This creates a disk of moons around the planet reaching out to $\sim 200R_J$, or roughly 0.1 AU from the planet. This distance sits well within the planet’s initial Hill radius of ~ 0.7 AU, which ensures the initial moon orbits are stable. (In this paper, we will not refer to the moon orbital distances in terms of the Hill radius because the Hill radius

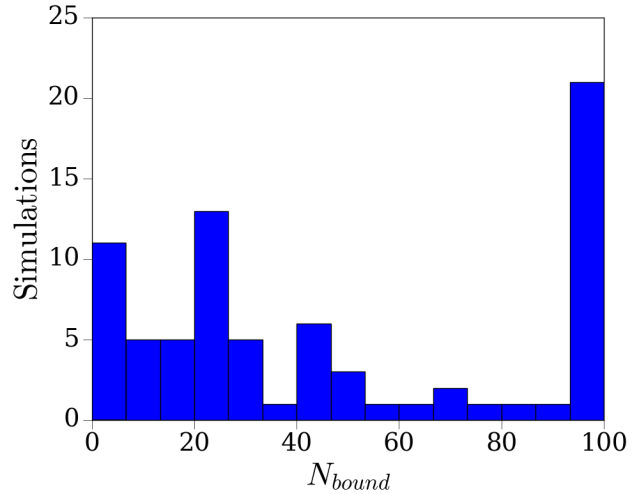


Figure 1. Distribution of the number of moons that remain bound to the ejected planet, N_{bound} . Most simulations retain a few to several moons after ejection while just over 25% of the simulations retain all or most of their moons. Systems that retain the majority of their moons likely had retrograde encounters with the perturbing planet, thus shortening the duration of the interaction and limiting the change in the moon’s velocity.

will change throughout the simulations as the orbits of the planets evolve.) This disk of moons is introduced with no inclination relative to the Cartesian coordinate system used by REBOUND—generally placing the disk at a slight angle relative to the planet’s orbit.

We note that our initial plan was to use REBOUND’s Simulation Archive to put the moons in place assuming that the planetary orbits would remain unchanged. However, the addition of the moons into the system forced the integrator to adjust its timestep to a smaller value, which caused the orbits of the planets to diverge from their moonless orbits. This change in timestep caused our escape rate to be less than 100 percent. Nevertheless, this method still produces a sufficient fraction of escaping systems. Thus, we continued with this approach and analyzed the planetary escapes that resulted—examining the orbits of the moons that remain around the ejected planet, as well as the fate of moons that were ionized from the planet but that remain in the stellar system.

3 RESULTS

We ran a total of 77 simulations with escaping planets over the course of this experiment and found that 47% of the moons remain bound to the escaping planets at the end of the simulation. An additional 22% of the moons were stripped from the planet, but remained bound to the star. The remaining 31% were stripped from both the planet and the star.

Figure 1 shows the distribution of the number of moons that were retained by the escaping planet. We see from this figure that the distribution of orbital distances of surviving moons is bimodal. Figure 2 shows the survival rate for the moons as a function of the moon’s initial distance from the

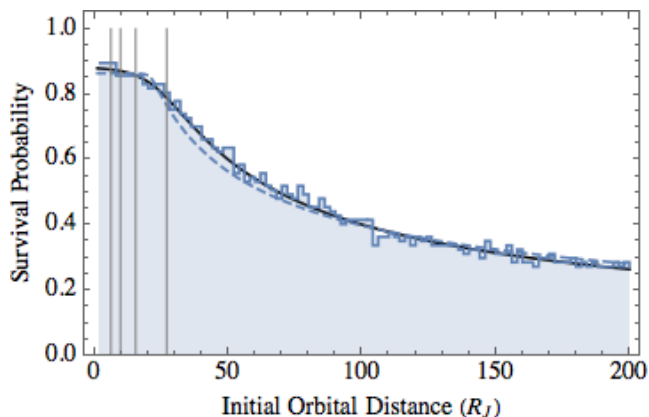


Figure 2. Fraction of surviving moons as a function of the moon’s initial distance from the parent planet. The vertical lines indicate the orbital distances of the Galilean moons, where a large majority of moons survive. The results of two, broken power-law fits to the data are shown. The blue dashed line had a fixed power-law index of $-1/2$. The solid black line is an improved fit with an index of roughly -0.6 .

planet. In general, the scattering events strip the outermost moons from the system and most systems lose some moons. However, a substantial fraction of the systems retain all of their moons. (Recall that these are non-interacting, test particle moons. A physical system of 100 interacting moons is unlikely to survive unscathed). Also shown in Figure 2 are the locations of the Galilean satellites of Jupiter. We see from this figure that a large fraction of the moons ($\sim 85\%$) near the orbits of the Galilean satellites will survive the ejection of the planet from the system.

The overall shape of the distribution in Figure 2 can be modeled as a broken power law with a constant value for small semi-major axes and a power-law tail for larger values. The tail scales approximately like $a^{-1/2}$, however, a far superior fit to the data occurs when the power-law index is left as a free parameter. A least-squares fit to the logarithm of the survival probability as a function of the logarithm of the semi-major axis yields an index of -0.607 ± 0.017 .

While many of the moons survive after the planet ejection, their orbits are often significantly disrupted. Figures 3(a), 3(b), and 3(c) show the distributions of the semi-major axes, eccentricity, and inclination for the surviving moons, while Figures 3(d), 3(e), and 3(f) show 2-dimensional plots of these elements. In these figures, moons are shown at their final orbital configuration with orbital elements calculated in reference to the host planet. We show only moons that have remained bound to the planet.

A few features stand out in these figures. A large fraction of the surviving moons have nearly circular orbits with the remainder of the eccentricities spread throughout the allowed range. The distribution of semi-major axis of the remaining moons also spans the entire range of the initial conditions. The orbits of the moons are reordered somewhat (as can be seen by comparing the final distribution in Figure 3(a) to the initial distribution in Figure 2) but most moons stay relatively close to their initial orbits. The final orbital inclinations are generally modest but the distribu-

tion is quite wide and extends to both polar and retrograde orbits in the most extreme cases. We assume the inclinations are often excited because the planets are first scattered into inclined orbits before being ejected from the system—which initiates stellar-induced changes to the inclination of the moon systems.

Another striking feature is the occasional, coherent pattern in the inclination of the surviving moons from several of the ejected planets. Systems that show these patterns generally retain most or all of their moons and can be identified in Figure 3 by observing distinct patterns to their final moons. These structures are caused by the precession of their orbits induced by the central star. Once a planet is scattered out of the plane of its initial orbit, the orbits of all of the moons become misaligned from the orbit of the planet around the star. The gravitational interaction between the star and the moons causes them to precess at different rates—producing those patterns. In some cases, the patterns develop in initial scattering events, but the subsequent planet-planet encounters eventually cause the planetary ejection will remove multiple moons—leaving partial precession patterns or disrupting them completely.

This pattern in inclination for an example system is shown in Figure 4, along with the longitude of ascending node Ω for the moon system. In this figure, the full precession structure can be seen. Large changes in the value of Ω indicate where its value completes a circuit of 2π and where its inclination is 0° .

We do not explore the cause of the high retention rate in these systems in this work. However, we suspect that the systems that retain the majority of their moons experienced scattering events that were retrograde with respect to the moon orbits. Since the velocity imparted to the moons is proportional to the crossing time of the encounter, it will be inversely proportional to the relative velocity of the moon and the perturber:

$$\Delta v_{\text{moon}} = \frac{F_G}{m_{\text{moon}}} \Delta t \simeq \frac{Gm_p}{b\Delta v} \quad (1)$$

where Δv_{moon} is the velocity imparted to the moon, F_G is the force of gravity (with Newton’s constant G), Δt is the passage time, m_p is the mass of the perturbing planet, b is the distance of closest approach (also assumed to be the crossing distance), and Δv is the difference between the velocities of the moon and the perturbing planet. In a prograde encounter, the moon and perturber are traveling in the same direction, yielding a small relative velocity, a long crossing time, and a large change to the velocity of the moon. In a retrograde encounter, the moon is traveling in the opposite direction, producing a large Δv , a small crossing time, and a small perturbation to the moon’s velocity. We inspected several systems where all of the moons were retained and each had primarily retrograde encounters—supporting our hypothesis. Nevertheless, a comprehensive exploration of this issue may prove interesting.

We note that the distribution of i measured in Figure 3(c)—as well as in the preceding paragraphs—is created in reference to the initial coordinate system of REBOUND. However, as the inclinations of the moons in the moon system vary over time we can consider how they are distributed about a mutual orbital plane. We define the mutual orbital plane to be the plane perpendicular to the total angular

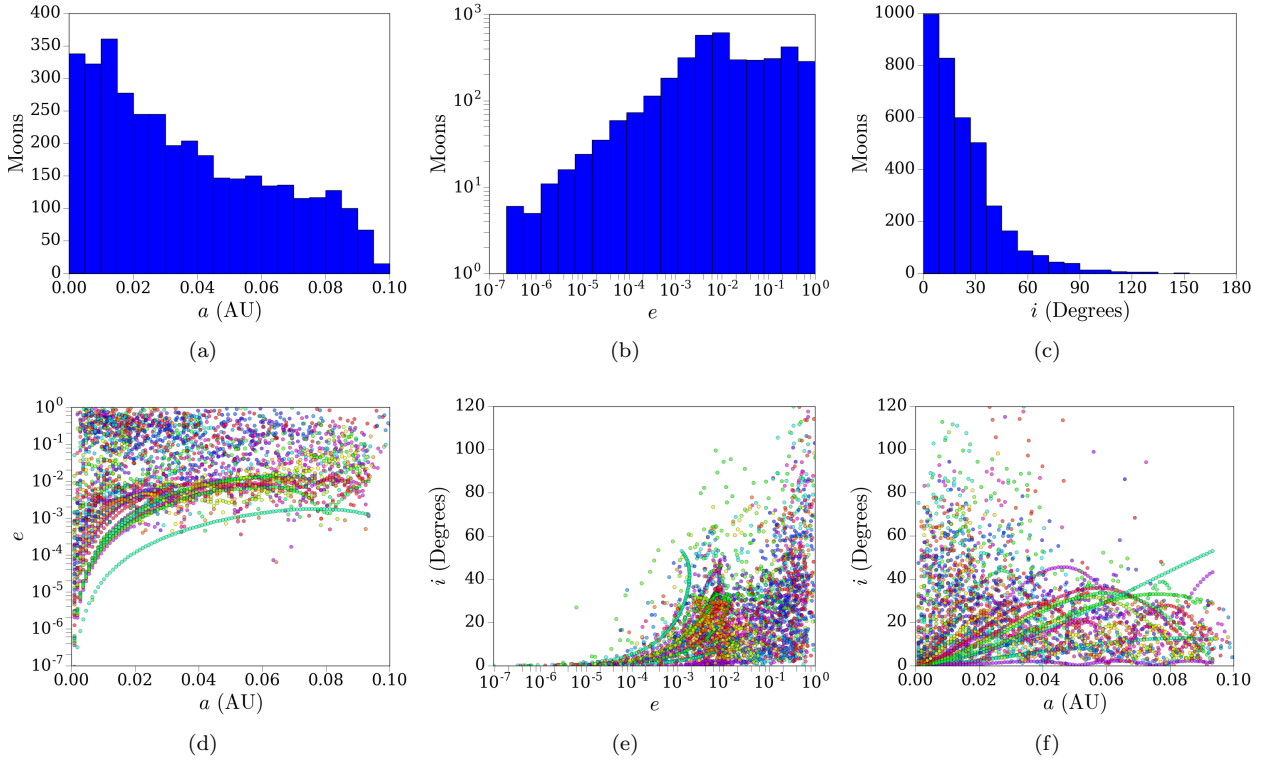


Figure 3. Top Row: The distributions of the final orbital elements (a , e , and i) of the moons that survive the planetary ejection. Eccentricity is plotted on a log-log scale. Bottom Row: Scatter plots of pairs of final orbital elements of the moons that survive the planetary ejections. In both sets of figures we see that the eccentricity distribution of the final moons has two clusters of points, one near 10^{-2} composed largely of the systems that retain the majority of the moons and the second with eccentricities of a few tenths. The coherent structures in the bottom panels are the result of precession in the moon orbits as the planet is perturbed onto an inclined orbit prior to being ejected from the system.

momentum vector of all of the moons that remain bound to the planet. We recalculate the inclination distribution with respect to this new orbital plane and show it in Figure 5. Distributions of individual systems are also shown in that figure, where a variety of spreads are seen from system to system depending upon the angle between the initial moon disk and the orbit of the host planet prior to its ejection. Figure 5 shows the inclination distribution when combined over all simulations and suggests that, when measured against their common orbital plane, moons are likely to have a nonzero value for i_{new} . Examining individual simulations shows that i_{new} is nonzero even at small orbital distances from the planet.

Ultimately, however, the visual aspect of these patterns are an artifact of our simulation setup since real moon systems are not this regular in their orbital properties—and the moons are not massless. One could imagine seeing the effects of such precession in a hypothetical, if unlikely, statistical study (of moons orbiting rogue planets or planets whose orbit are highly inclined with respect to other planets in the same system). Other effects that we do not consider here, such as planet oblateness, moon mass, and formation processes, will also contribute to the architecture of the surviving moon systems. Thus, our distributions of inclination, eccentricity, and semi-major axis are best viewed as the parameter space where the orbits of individual moons would be found and not necessarily how moons with in a particular

system would relate to each other. Nevertheless, we expect the bulk properties of the surviving moon distribution to roughly match these results.

An interesting question to consider on similar statistical grounds is whether or not resonant orbits can survive the ejection process. Mean-motion resonances are common among moon systems in the solar system, and would presumably be common in moon systems of extrasolar planets (e.g., [Murray & Dermott 1999](#)). Thus, we examine the effects that planet-planet scattering has on such resonant dynamics (now using massive moons) in section 5.

4 MOONS THAT ARE LEFT BEHIND

Our systems produced a large population of moons that are stripped from their host planet, but that remain bound to the star. Figure 6 shows the orbital elements of these moons (calculated with respect to the initial coordinate system of the simulation). Figure 6(b) shows a correlation in the eccentricity distribution—a larger number of moons have high eccentricity. This feature is, in part, a consequence of the fact that our planetary orbits are at a few AU, while the escape distance is 100 AU. Thus, the scattering happens close to the Sun (where the future pericenter of the final orbit will be), but the moons can have semi-major axes that are much larger—producing a large apocenter.

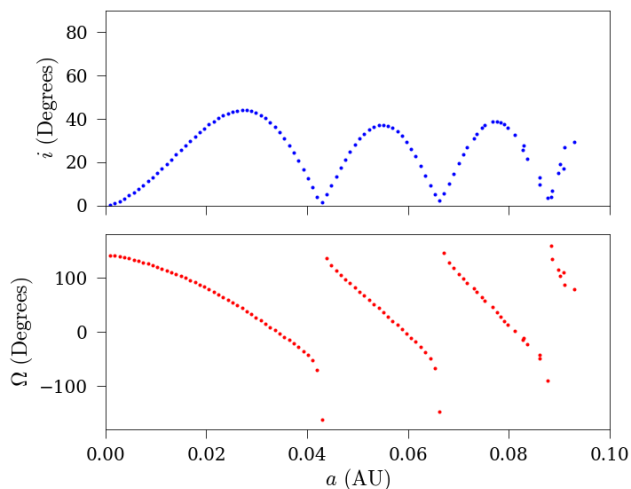


Figure 4. Graph of inclination and longitude of ascending node for moons in a simulation that retained all of its moons. Orbital elements are taken 10^6 days after the moons are first added. Points of 0° inclination (blue) coincide with large changes in Ω (red) where the orbital elements cycle from -180° to $+180^\circ$.

The inclination distribution in Figure 6(c) shows that moons span the full range of values from 0 to 180 degrees. Most moons have only modest inclinations of a few tens of degrees. Nevertheless, roughly 30% of the simulated moons have an inclination at or above 90 degrees—occupying polar or retrograde orbits around the star.

5 MEAN-MOTION RESONANCES

Another important effect we consider, especially when imagining the potential to harbor life, is whether or not the details of the dynamical state of a moon system remains—specifically the resonance behavior. Without a perturbing body, the orbit of the moon would circularize, removing an essential ingredient for tidal heating (Yoder & Peale 1981)—though a spin-orbit coupling other than 1:1 would allow eccentricity to persist (as is the case with Mercury’s eccentricity of 0.2). And, while nonresonant configurations can induce a forced eccentricity in the orbits of the moons, they would generally be quite small (of order the moon/planet mass ratio) since the conjunctions that produce the eccentricities occur randomly about the orbit. Either way, the resonant configuration of Jupiter’s Galilean moons plays an important role in keeping the eccentricities of Io and Europa large enough to allow tidal heating to warm their interiors (Yoder 1979).

Capturing two moons into mean-motion resonance beginning from a non-resonant configuration usually requires that their orbital period ratio converges from a larger value to the resonance value (Peale 1976; Lee & Peale 2002). This situation can arise in the presence of the disk from which the moons form—where the disk dissipates the orbital energy of the outer moon faster than it does the inner moon. Without a disk it may still be possible to produce a resonant configuration through convergent migration (e.g., by the tidal decay of an exterior moon on an eccentric orbit). For lunar

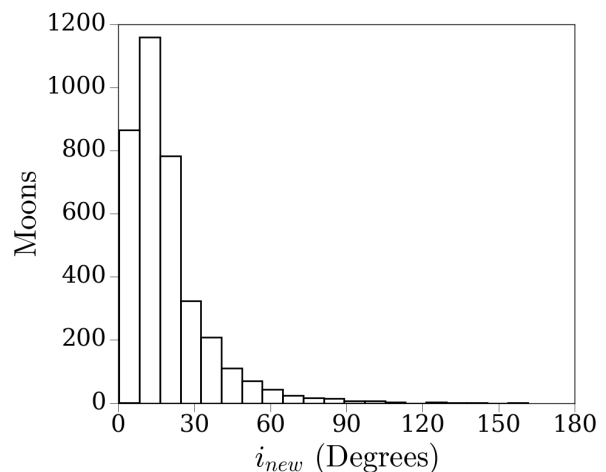
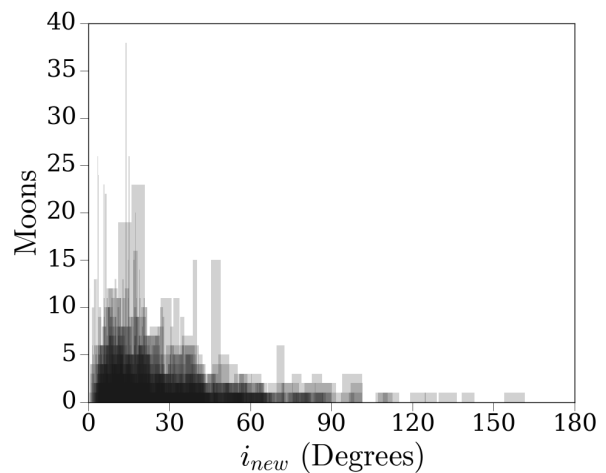


Figure 5. Inclination distributions of surviving moons with respect to their common orbital plane (defined by the direction of the total angular momentum of the moons). Top: Distributions of individual simulations. Darker regions correspond to values that are densely occupied by surviving moons. Bottom: The combined distribution from data collected over all simulations. The peak inclination is distinctly nonzero in these distributions.

orbits around a rogue planet, the most straightforward way to generate a resonant configuration is by simply to preserve that configuration throughout the ejection process.

To see if resonances can survive ejection, we replace the disk of moons described in Section 2 with two different sets of resonant moon systems. The first set uses two-moon systems in a 2:1 orbital resonance. The second set uses three moon systems in the three-body, Laplace resonance. These moons are one lunar mass each, and are positioned at the orbital distances of Io, Europa, and Ganymede from the planet. Once positioned, the simulation is integrated to the planetary escape as normal. For all systems, we record the 2:1 resonant argument, $\phi = \lambda_1 - 2\lambda_2 + \varpi_1$, of the inner planet pair as it evolves over the simulation time. In a sustained 2:1 resonance, this value oscillates around 0° . For the Laplace resonance systems, we record the 2:1 resonances between the outer pair of moons and the Laplace resonant argument $\Phi_L = \lambda_1 - 3\lambda_2 + 2\lambda_3$, which oscillates about 180° .

We run 10 simulations from each set (the 2:1, two-

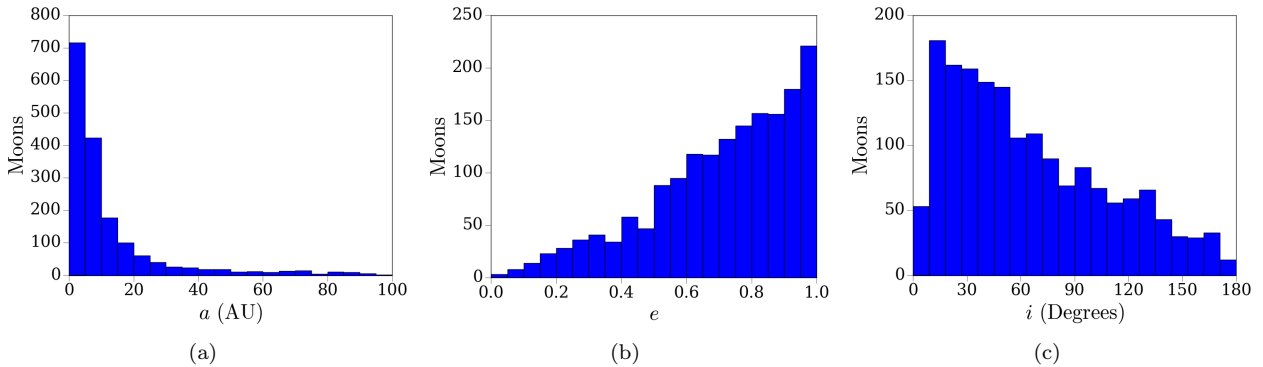


Figure 6. Distribution of a , e , and i for moons that are unbound from their host planet, but remain bound to the central star. Elements are calculated with respect to the system’s center of mass, and with respect to the simulation’s initial coordinate system. The majority of these remnant moons have small orbital distances (compared with our ejection criterion of 100AU). These moons favor large values of eccentricity and inclination—including a large fraction of polar and retrograde orbits.

moon and the Laplace, three-moon configurations), with the moons starting in their respective resonances. Following the ejection of the planet from the system, the resonant arguments continue to oscillate in seven of the 10, 2:1 resonance simulations. Eight of the 10 Laplace resonance simulations retain some resonance behavior—six keep the Laplace resonance, one system keeps the individual 2:1 resonances, but not the Laplace resonance, and one keeps the inner 2:1 resonance but not the outer resonance. These results show that resonances are often retained throughout the ejection process. These numbers are also consistent with the overall moon survival rate near the Galilean moon orbital distance seen in Figure 2.

As an example, we show the evolution of a Laplace resonance system in Figure 7, where each of the three resonant arguments is plotted over the entire simulation time (t_{sim}). We see in this figure that the ejection process can have very little effect on the dynamical state of the moon system—even though several encounter events occur before the planet finally leaves the system near the end of the time series. These simulations demonstrate the potential survival of a resonant moon configuration through the ejection of the host planet—and therefore the potential that such resonant configurations may exist about rogue planets. Subsequent evolution of the moons’ orbits through tidal interactions may restore the Laplace resonance at a future time (Deienno et al. 2014).

We also note that moons that stay in resonance also maintain a common orbital plane throughout the simulation—though the orientation of this plane can shift over time. Some simulations in resonance produce coplanar moon systems with large inclinations by the time the host planet is ejected—up to 60° from their initial configuration in the largest cases. For real systems, if the orbits become too inclined, the resonances may be affected by the oblateness of the host planet.

Our initial set of resonance systems had moons near the orbits of the Galilean satellites—quite close to the host planet where a large fraction of the orbits survive (Figure 2). We also tested resonance configurations in larger initial orbits where lunar ionization is more likely to occur. For these simulations, we move the inner moon out to either $40R_J$ or

$75R_J$ —giving them a typical survival rate of ~ 0.7 and ~ 0.5 , respectively (as estimated from Figure 2). We then place a second moon outside the first to create a 2:1 resonance. Ten simulations are run for each orbital distance. For the $40R_J$ suite, four of the 10 simulations maintain the 2:1 resonance, while another two simulations retain both moons but lose the resonant interaction. This results in a total of ten surviving moons out of the initial 20—slightly less than what we would expect from the test particle simulations. For the $75R_J$ suite, a total of five moons are retained across all 10 simulations (25%), but no resonant configurations survive. Thus, while resonant orbits can survive the ejection process—even on orbits larger than the Galilean satellites—a larger fraction of the moons will be lost. Moreover, the resonances are (not surprisingly) more fragile than the individual orbits of the moons.

6 COMPARISON WITH OTHER WORK

Our results share similarities with Hong et al. (2018), a recent work which also examined the dynamics of moons during close planetary encounters¹. We focus primarily on the effects that planet ejection has on the survivability of moons and the evolution of their orbital configuration. Thus, we only consider the moons that orbit the planet that is eventually ejected from the system and our initial conditions concentrate our moon sample closer to our planet than what was done in Hong et al. (2018). The planetary systems in both works are similar—a star orbited by three planets. They used a variety of planet masses (chosen from 0.1, 0.3, 0.5, and 1.0 M_J), studied moons that were orbiting all of the planets out to distances of 1/2 of the Hill radius (compared to 1/7 for this study), and modeled the effects of oblateness.

Comparing the moon survival rate in Figure 2 to the corresponding results (Hong et al. (2018), Figure 5), we find a survival rate vs. distance relationship that is larger as a

¹ We became aware of the independent work of Hong et al. (2018) as we prepared to present our initial results at the January 2018 meeting of the American Astronomical Society, (Rabago & Steffen 2018).

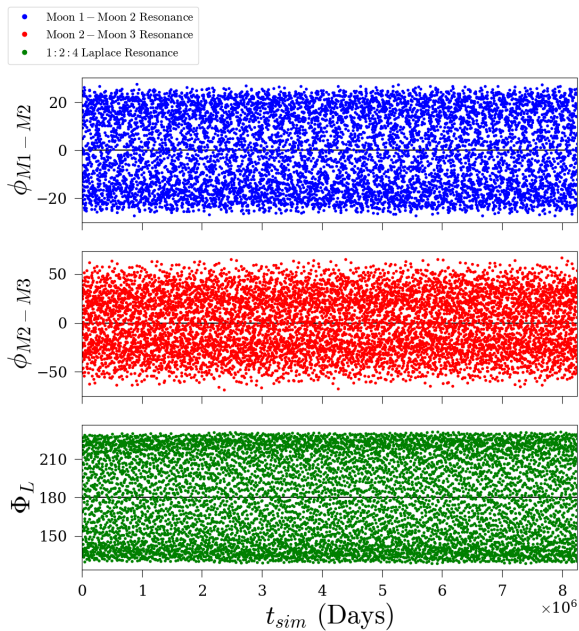


Figure 7. Resonance angles as a function of time for the two 2:1 (top and middle) and the Laplace (bottom) resonances for one of our Laplace resonance, three-moon systems. The time series spans the entirety of the simulation, including the ejection of the host planet from the system. This result shows that the resonance behavior of the system can be preserved throughout the evolution of the system and will persist after the host planet leaves the system. Thus, the conditions on the Galilean satellites (such as volcanoes on Io and liquid water on Europa) could persist on rogue planets for billions of years.

whole, and decays at a slower rate with distance. Most of the differences between our results can result from the differences in our initial system properties. Smaller mass perturbers will require more close encounters before a planet can be ejected—implying more scattering events and its accompanying potential for losing additional moons. Moons on larger orbits are easier to ionize from the host planet. And, lower-mass planets are likely to lose more moons when perturbed by larger counterparts.

7 CONCLUSIONS

We have shown that giant planet scattering events will not completely disrupt moon systems even when the host planet is ejected from the system. Our results predict a population of exomoons orbiting rogue gas giant planets. These moons survive to a considerable distance from the host planet ($\gtrsim 200R_J$). The various encounters leading up to planetary escape leave the surviving moons in a wide range of orbital parameter space. We see that precession, caused by planet-sun and planet-planet interactions, can excite the mutual inclinations of the moons in a system. Nevertheless, the moon systems can often retain key dynamical properties.

Some moons that are stripped from the planet will remain bound to the star in heliocentric orbits. Many of these moons are in smaller, eccentric orbits, with a significant fraction of moons occupying high inclinations. Over

long timescales such moons would likely interact with the remaining planets in the system and either be ejected, or collide with the central star or planets. Some fraction, after additional scatterings that bring their pericenter distances closer to the star, may have their orbits decay through tidal dissipation—placing them on very short orbits and possibly contributing to the population of ultra short period planets (Sanchis-Ojeda et al. 2014; Steffen & Coughlin 2016).

Although we used Jupiter-mass planets in these simulations, similar scenarios can occur with lower mass planets, such as Saturn or Neptune-mass planets. Although a detailed study on the effect of planetary masses is beyond the scope of this project, we expect lower-mass planets to require more encounters prior to a planetary ejection possibly producing a smaller range in values for remaining moons due to the multiple encounters. Nevertheless, certain features, such as the inclination-precession behavior of bound moons in circular orbits, are expected to remain as the cause of these features is independent of the host planet mass.

We find that resonant interactions can persist through planetary escape. In our simulations, moon systems that maintained their resonance behavior did not undergo large excitations to their eccentricities, and were able to remain coplanar despite the influences from the star and other planets. These results, along with the survival rate shown in Figure 2, imply a significant fraction of escaping planets can retain a resonant moon system.

An important consequence of our results is that moons like the Galilean satellites, which are geologically active and can sustain subterranean liquid water, could exist around rogue planets. Moreover, since the mechanism that sustains the liquid water (tidal heating) can persist for billions of years, it raises the significant possibility for life to develop or persist around these planets in the absence of a host star. Thus, lunar systems around rogue planets may constitute a new reservoir for life. If a significant fraction of hot Jupiter systems are formed by planet-planet scattering (hot Jupiters exist around roughly 1% of stars (Wright et al. 2012)), then the number of potential life-harboring rogue planets could be hundreds of millions or billions across the galaxy.

ACKNOWLEDGEMENTS

Simulations in this paper made use of the REBOUND code, which can be downloaded freely at <http://github.com/hannorein/rebound>. The author would like to thank Hanno Rein for his assistance with some of the finer points of the REBOUND integrator. We acknowledge support from NASA grants NNX16AK32G and NNX16AK08G. We also thank Benjamin Bromley for useful discussions.

REFERENCES

- Bennett D. P., et al., 2014, *ApJ*, **785**, 155
- Chatterjee S., Ford E. B., Matsumura S., Rasio F. A., 2008, *ApJ*, **686**, 580
- Deienno R., Nesvorný D., Vokrouhlický D., Yokoyama T., 2014, *AJ*, **148**, 25
- Forgan D., Kipping D., 2013, *MNRAS*, **432**, 2994
- Goldreich P., Soter S., 1966, *Icarus*, **5**, 375

- Hinkel N. R., Kane S. R., 2013, *ApJ*, **774**, 27
- Hong Y.-C., Raymond S. N., Nicholson P. D., Lunine J. I., 2018, *ApJ*, **852**, 85
- Knutson H. A., et al., 2014, *ApJ*, **785**, 126
- Lammer H., et al., 2014, *Origins of Life and Evolution of the Biosphere*, **44**, 239
- Lee M. H., Peale S. J., 2002, *ApJ*, **567**, 596
- Murray C. D., Dermott S. F., 1999, *Solar system dynamics*
- Peale S. J., 1976, *ARA&A*, **14**, 215
- Rabago I., Steffen J. H., 2018, in *American Astronomical Society Meeting Abstracts #231*. p. 148.23
- Rasio F. A., Ford E. B., 1996, *Science*, **274**, 954
- Rein H., Liu S.-F., 2012, *A&A*, **537**, A128
- Rein H., Spiegel D. S., 2015, *MNRAS*, **446**, 1424
- Rein H., Tamayo D., 2017, *MNRAS*, **467**, 2377
- Reynolds R. T., McKay C. P., Kasting J. F., 1987, *Advances in Space Research*, **7**, 125
- Sanchis-Ojeda R., Rappaport S., Winn J. N., Kotson M. C., Levine A., El Mellah I., 2014, *ApJ*, **787**, 47
- Schlaufman K. C., Winn J. N., 2016, *ApJ*, **825**, 62
- Sparks W. B., Schmidt B. E., McGrath M. A., Hand K. P., Spencer J. R., Cracraft M., E Deustua S., 2017, *ApJ*, **839**, L18
- Squyres S. W., Reynolds R. T., Cassen P. M., 1983, *Nature*, **301**, 225
- Steffen J. H., Coughlin J. L., 2016, *Proceedings of the National Academy of Science*, **113**, 12023
- Sumi T., et al., 2011, *Nature*, **473**, 349
- Vance S. D., et al., 2018, *Journal of Geophysical Research (Planets)*, **123**, 180
- Wright J. T., Marcy G. W., Howard A. W., Johnson J. A., Morton T. D., Fischer D. A., 2012, *ApJ*, **753**, 160
- Yoder C. F., 1979, *Nature*, **279**, 767
- Yoder C. F., Peale S. J., 1981, *Icarus*, **47**, 1
- Zollinger R. R., Armstrong J. C., Heller R., 2017, *MNRAS*, **472**, 8

This paper has been typeset from a $\text{\TeX}/\text{\LaTeX}$ file prepared by the author.